Journal of Alloys and Compounds 509 (2011) 2386–2391

Contents lists available at ScienceDirect

Journal of Alloys and Compounds

journal homepage: www.elsevier.com/locate/jallcom

The effect of chromium (III) oxide (Cr_2O_3) nanopowder on the microstructure and cyclic hydrogen storage behavior of magnesium hydride (MgH_2)

Marek Polanski[a], Jerzy Bystrzycki[a], Robert A. Varin[b,*], Tomasz Plocinski[c], Marcin Pisarek[c]

[a] Faculty of Advanced Technology and Chemistry, Military University of Technology, 2 Kaliskiego Str., 00-908 Warsaw, Poland
[b] Department of Mechanical and Mechatronics Engineering, University of Waterloo, 200 University Ave. W., Waterloo, Ontario, Canada N2L 3G1
[c] Faculty of Materials Science and Engineering, Warsaw University of Technology, 141 Woloska Str., 02-507 Warsaw, Poland

ARTICLE INFO

Article history:
Received 11 October 2010
Accepted 3 November 2010
Available online 10 November 2010

Keywords:
Solid state hydrogen storage
Ball milling
Magnesium hydride (MgH_2)
Chromium oxide (Cr_2O_3)
Cycling
Microstructure

ABSTRACT

High energy ball milling in a Fritsch P6 planetary ball mill was used for the synthesis of the nanocomposite of MgH_2 with 10 wt.% of Cr_2O_3 nanopowder catalyst (particle size <50 nm). After ball milling for 1 h the resulting grain size of β-MgH_2 was equal to ~30 nm. Subsequently, the nanocomposite was subjected to 150 desorption/absorption cycles at 325 °C. A gradual loss of hydrogen storage capacity upon cycling from ~5.2 wt.% after 1 cycle to ~4.6 wt.% after 150 cycles is observed on respective PCT curves obtained at 325 °C after every 25 cycles. The TPD curves temperature maxima are gradually shifted to a higher temperature range with increasing number of cycles which may indicate a lowering of the overall rate of transformation. Thorough microstructural investigations using such techniques as X-ray diffraction (XRD), scanning transmission electron microscopy (STEM) and X-ray photoelectron spectroscopy (XPS) of the samples after 150 cycles of desorption/absorption show profound microstructural changes such as sintering of individual powder particles into agglomerates, increase in grain/crystallite size (>100 nm), segregation of the Cr_2O_3 particles to the interfaces between the sintered Mg particles and some reduction of Cr_2O_3 to Cr and MgO. All these microstructural changes seem to be responsible for the reduction of hydrogen storage capacity upon cycling and lowering the overall rate of transformation.

1. Introduction

The general service conditions of an advanced proton exchange membrane (PEM) fuel cell stack which is a primary candidate for automotive applications require hydrogen pressure of about 1.1–1.8 bar while the generated temperature usually does not exceed 60–70 °C [1]. In view of this, it has been widely realized that high temperature metallic/intermetallic hydrides, particularly those based on Mg, are not suitable hydrogen storage materials for supplying a PEM fuel cell stack. For example, a serious thermodynamic constraint for magnesium hydride (MgH_2) is its high enthalpy of formation/decomposition which is within the range of 71–75 kJ/mol [2] and does not allow dehydrogenation below about 280 °C at 1 bar H_2 (atmospheric pressure). No catalytic additive is able to alter this unfavorable thermodynamics.

However, as first reported by Bogdanović et al. [3,4] this disadvantageous thermodynamics of the MgH_2–Mg system for a solid state hydrogen storage can be quite advantageous for heat storage because approximately 0.9 kWh of heat per kg Mg can be stored at a hydrogen-pressure-dependent temperature level between 300 and around 500 °C applicable for solar power generation via Stirling engines or storage of industrial heat in the above temperature ranges.

Since those pioneering works of Bogdanović et al. a huge number of articles have been published on the entire spectrum of catalytic additives which can enhance absorption/desorption rate of the Mg–MgH_2 system which were recently critically reviewed in [2]. One group of catalytic additives is based on metal oxides especially in the form of nanopowders. Most recently, we reported a very good catalytic effect of nanometric Cr_2O_3 (particle size <50 nm) on the acceleration of the absorption/desorption kinetics of ball milled MgH_2 [5].

The present paper reports the results of further studies on the effect of nanosized Cr_2O_3 on cyclic (desorption/absorption) behavior of ball milled MgH_2 + 10 wt.% Cr_2O_3. A thorough understanding of the microstructural and accompanying hydrogen storage property changes is of fundamental importance for further development of MgH_2 as a potential material for thermochemical thermal energy storage. As argued by Klassen [6] MgO is more stable than all effective oxide catalysts and provides the lowest chemical potential for oxygen. Based on thermodynamics, a complete reduction of the TM oxide by Mg is expected, forming TM and MgO. However, this is generally not observed during milling but can be accelerated

* Corresponding author. Tel.: +1 519 888 4567; fax: +1 519 885 5862.
E-mail addresses: ravarin@mecheng1.uwaterloo.ca, ravarin@uwaterloo.ca (R.A. Varin).

0925-8388/$ – see front matter © 2010 Elsevier B.V. All rights reserved.
doi:10.1016/j.jallcom.2010.11.026

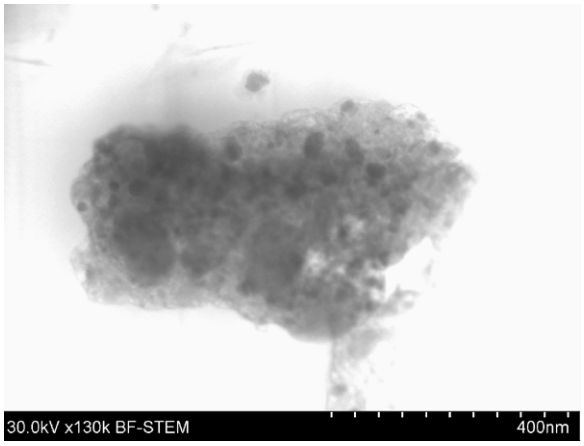

Fig. 1. A bright field (BF) image obtained in the STEM mode of an individual ball milled powder particle of the MgH_2 + 10 wt.% Cr_2O_3 nanocomposite without thinning with FIB.

during cycling of MgH_2 containing a nanometric oxide catalyst. Hence, that would reduce the overall hydrogen capacity due to the formation of MgO and also degrade the Cr_2O_3 catalyst. The present results show that the degradation of the Cr_2O_3 catalyst during cycling at 325 °C up to 150 desorption/absorption cycles is only one of many other microstructural changes occurring during cycling.

2. Experimental

Magnesium hydride (MgH_2) powder (98%) was purchased from ABCR GmbH & Co. KG, trade name MG-5026; ABCR Germany. Chromium (III) oxide (Cr_2O_3) nanopowder (particle size <50 nm) was supplied by Sigma–Aldrich. 5 g of the MgH_2 + 10 wt.% Cr_2O_3 mixture together with 5 mm diameter stainless steel balls weighing 120 g and 7 ml of an inert hydrocarbon were sealed together in an 80 ml stainless steel vial under high purity argon of min. purity of 99.999% (H_2O and O < 1 ppm) and milled in a Fritsch P6 planetary ball for total time of 1 h with a rotation speed of 650 rpm under high purity argon with. After milling the handling of powders was conducted in a Labmaster glovebox station filled up with high purity argon. The amounts of oxygen and water were below 0.1 ppm.

A sample of about 100 mg was subjected to desorption/absorption hydrogen cycling in HTP1-S (Hiden Isochema) Sieverts type sorption analyzer. The desorption step in cycling was conducted under high vacuum of 10^{-6} mbar at 325 °C. Absorption was conducted under 10 bar of hydrogen pressure. To evaluate precisely the amount of hydrogen absorbed by the sample, absorption isotherms were performed before cycling and after each 25 cycles. The total of 150 desorption/absorption cycles were conducted.

The X-ray diffraction (XRD) phase analysis before and after cycling was performed with a Seifert 3003 X-ray diffractometer using Co Kα radiation (λ = 1.79 Å) with operating parameters of 30 mA and 50 kV and a step size of 0.02°/5 s.

The morphology and microstructure of the investigated samples were examined with a high-resolution field emission scanning electron microscope (HITACHI S5500), equipped with a backscattered electron detector, an energy dispersive X-ray spectrometer (EDS) and a duo-STEM bright/dark field (BF/DF) detector. A transmission electron microscope (JEOL JEM 1200EX) with an accelerating voltage of 120 kV was also used to investigate microstructure and diffraction patterns for phase identification. Thin foils for scanning-transmission electron microscopy were prepared by the focused ion beam (FIB) technique using the FB-2100 Hitachi system. A liquid ion metal source was used as the source of the gallium ion beam at the accelerating voltage of 40 kV. Tungsten was used as a protective layer.

To determine the effect of cyclic hydriding/dehydriding on the decomposition temperature of cycled samples, the temperature programmed desorption (TPD) tests were performed by using the same HTP1-S analyzer coupled with a quadrupole mass spectrometer. The measurements were performed with heating rate of 20 °C/min under a high purity (99.999%) helium flow.

3. Results and discussion

3.1. Microstructure after ball milling

Fig. 1 shows a bright field (BF) image obtained in the STEM mode of an individual ball milled powder particle of the MgH_2 + 10 wt.% Cr_2O_3 nanocomposite. Dark features represent Cr_2O_3 particles which seem to be rather uniformly distributed in the MgH_2 matrix.

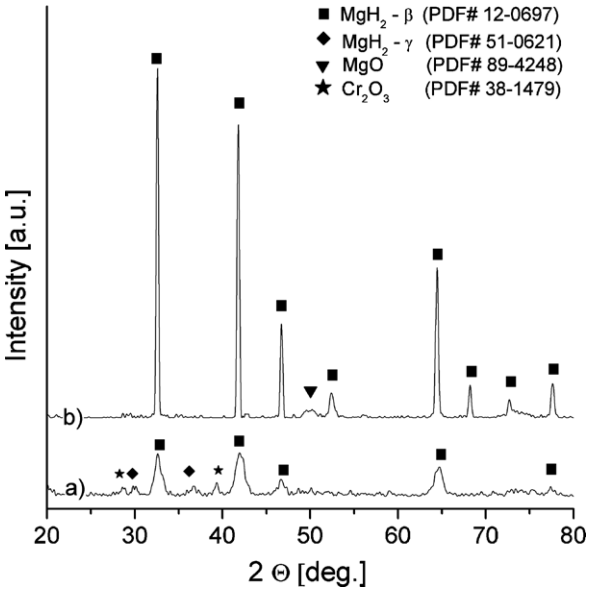

Fig. 2. XRD patterns of MgH_2 + 10 wt.% Cr_2O_3 composites after (a) high energy ball milling and (b) 150 desorption/absorption cycles (after final absorption). JCPDS file numbers for phase identification are given in the parenthesis.

The phase presence in the microstructure after ball milling is confirmed by an XRD pattern in Fig. 2a which shows primary diffraction peaks of an equilibrium and metastable β-MgH_2 and γ-MgH_2 phase the latter being a high pressure allotropic form of MgH_2 commonly found in ball milled microstructure of MgH_2 [2]. Weaker but still well discerned diffraction peaks of Cr_2O_3 are also observed. All peaks are rather broad indicating nanocrystallinity of the phases. The grain/crystallite size of β-MgH_2 was estimated as being equal to about 30 nm using the methodology described in detail in [5].

3.2. Hydrogen storage properties and microstructure after cycling

Fig. 3 shows hydrogen absorption pressure-composition-temperature (PCT) isotherms at 325 °C for samples subjected to a

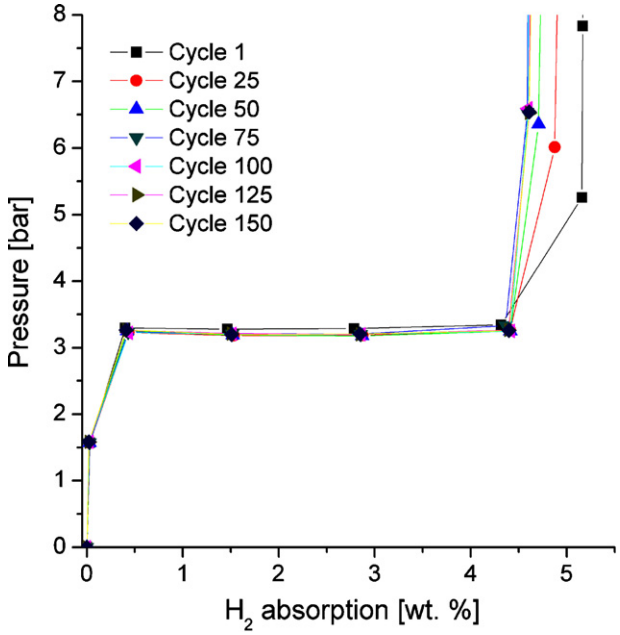

Fig. 3. Hydrogen absorption isotherms at 325 °C for samples subjected to a specified number of absorption and desorption cycles as indicated in the legend.

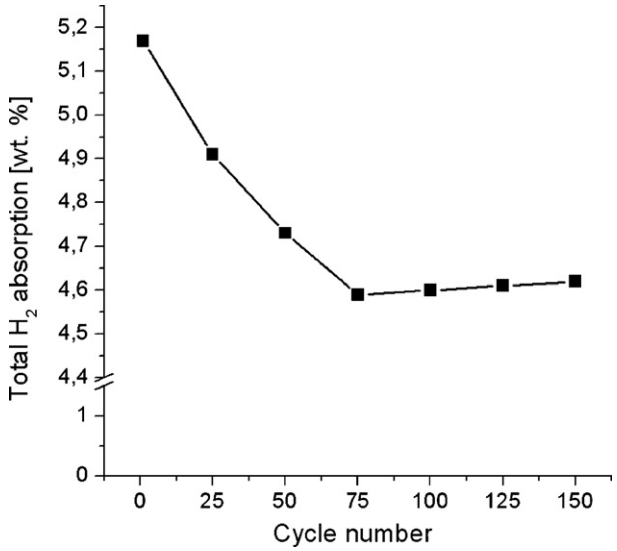

Fig. 4. The total hydrogen absorption capacity obtained from PCT curves (Fig. 3) after a specified number of cycles at 325 °C.

specified number of absorption and desorption cycles as shown in the legend. It is clearly observed that there is a systematic loss of hydrogen capacity with increasing number of cycles. The overall hydrogen capacity corrected for purity and oxide addition in MgH_2 + 10 wt.% Cr_2O_3 is ~6.7 wt.%. Fig. 4 shows that after only one cycle the total hydrogen capacity is reduced to about 5.2 wt.% and then it further decreases with increasing number of cycles reaching about 4.6 wt.% after 75 cycles. Quite unexpectedly, for the next 75 cycles the total hydrogen capacity is not affected by cycling and remains at a constant level of ~4.6 wt.%. This behavior strongly suggests that most of the microstructural changes that might be responsible for the capacity loss occur within the time duration equivalent to approximately the first 75 cycles. In general, the hydrogen capacity loss with the progressive cycling is quite commonly observed for ball milled MgH_2 both undoped and doped with catalytic additives [2,7]. This phenomenon for an undoped MgH_2 can be related to a progressive sintering of initial powder particles possibly accompanied by grain/crystallite growth of the Mg matrix within the sintered particles which could increase diffusion distances for hydrogen. Additionally, for MgH_2 containing Cr_2O_3 there may occur a gradual degradation of the Cr_2O_3 catalytic additive owing to its reduction by Mg and formation of MgO during an absorption step in cycling which may also reduce the hydrogen desorption/absorption rate and lead to the incomplete transformation of β-MgH_2 into Mg and vice versa.

Careful microstructural investigations were conducted in order to verify the principal microstructural changes which occurred during cycling in the present work. Fig. 5 shows a bright field (BF) STEM image of the microstructure of nanocomposite Mg + 10 wt.% Cr_2O_3 after desorption carried out after 150 cycles. Fig. 5a, taken at a lower magnification, clearly shows that individual Mg/MgH_2 particles produced after ball milling are, indeed, effectively sintered as a result of long term cycling. Fig. 5b, taken at a higher magnification, also shows that the Cr_2O_3 particles segregated to a certain extent during cycling to the interfaces between the sintered Mg particles. It is to be reminded that after ball milling Cr_2O_3 particles were initially quite uniformly distributed within the individual MgH_2 particles (see Fig. 1). Fig. 6 shows a high magnification transmission electron microscopy (TEM) image of the microstructure of the sample after 150 of desorption/absorption cycles. A corresponding selected area diffraction pattern (SADP) in the inset shows some

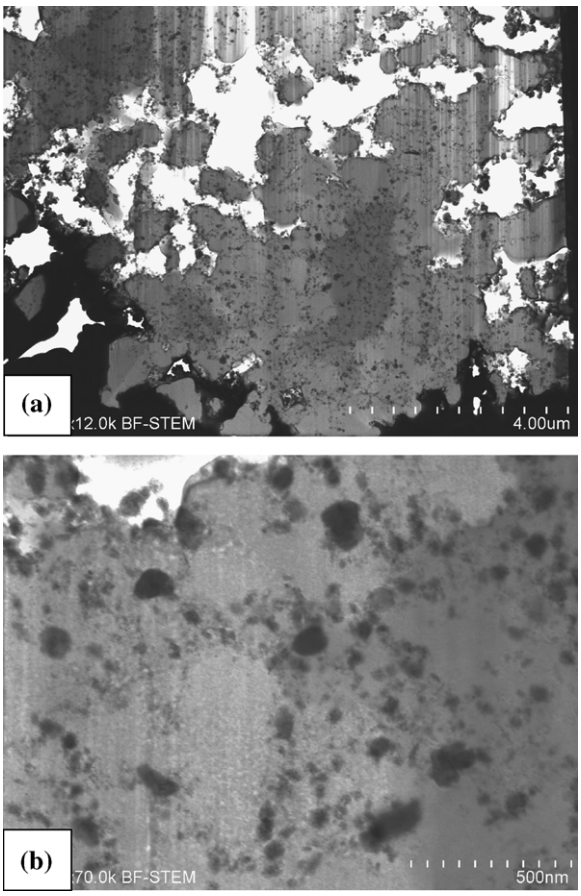

Fig. 5. BF-STEM image showing the microstructure of the nanocomposite Mg + 10 wt.% Cr_2O_3 after desorption conducted after 150 cycles as obtained from a thin foil produced by FIB: (a) a cross-section at a lower magnification and (b) higher magnification of a selected area.

poorly developed diffraction rings corresponding to the Mg matrix with superimposed diffraction spots of Mg. The appearance of such poorly developed diffraction rings strongly suggests that the average grain/crystallite size after 150 cycles must be larger than about 100 nm. The grain/crystallite growth during cycling is well documented in the literature. For example, Varin et al. [7] reported an increase of grain size of MgH_2 from ~30 nm recorded after

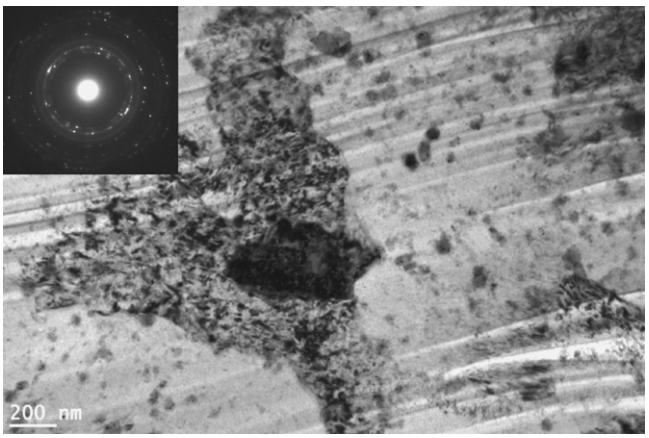

Fig. 6. High magnification transmission electron microscopy (TEM) image and corresponding selected area diffraction pattern (SAD) in the inset of a sample after 150 of desorption/absorption cycles.

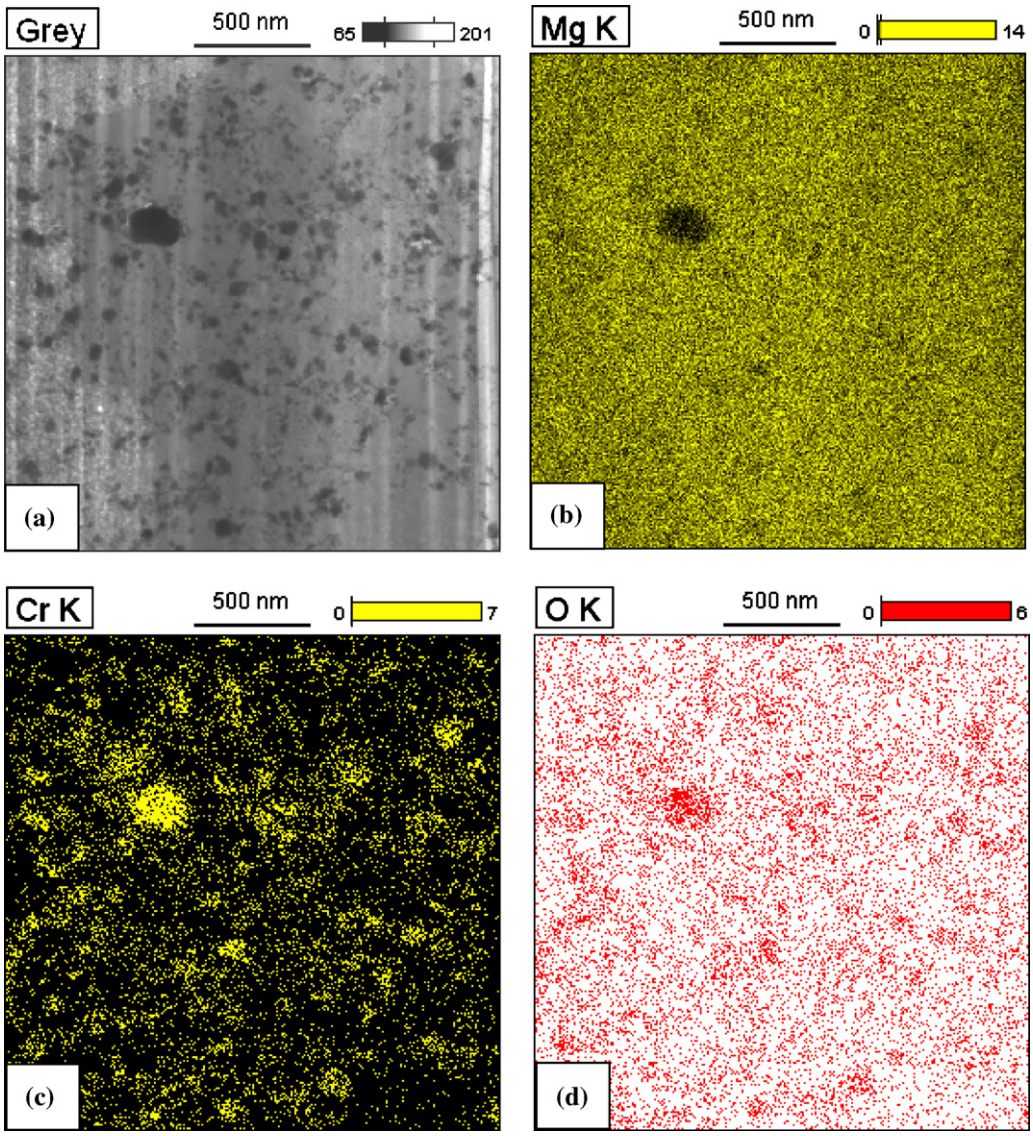

Fig. 7. (a) BF-STEM image and EDS maps showing the distribution of Mg (b), Cr (c) and oxygen (d) in the particle after 150 cycles from a thin foil obtained by FIB.

ball milling to 90 ± 10 nm after barely 5 cycles at 300 °C for MgH_2 originally doped with a nanometric Ni catalyst which was eventually transformed into an intermetallic/hydride Mg_2Ni/Mg_2NiH_4 as a result of cycling. Paik et al. [8] reported an increase of grain size of MgH_2 from ~60–70 nm recorded after ball milling to over 200 nm after only 6 cycles at 300 °C. However, in contrast to the results in the present work and those reported in [8], Dehouche et al. [9] reported that for the MgH_2 + 0.2 mol.% Cr_2O_3 the grains/crystallites of MgH_2 grew from initially from 21 nm for ball milled material to barely 84 nm after 1000 cycles at 300 °C. It is hard to explain such a low nanograin growth rate during so many thermal cycles at such a high temperature. However, it must be pointed out that in contrast to our experiments the cyclic loading carried out by Dehouche et al. [9] was performed at 300 °C under continues hydrogen pressure, i.e., the desorption pressure of 0.25 bar and absorption pressure of 10 bars. It might have influenced the grain growth of both Mg/MgH_2 phases.

Some bright spots arranged in a ring-like pattern in the SADP in Fig. 6 have been identified as corresponding to other phases such as Cr_2O_3, Cr and MgO. The presence of Cr and MgO suggests that a fraction of Cr_2O_3 was definitely reduced by Mg. In order to get more insight into the distribution of the elements in the Mg matrix of the material after 150 cycles an EDS mapping was carried out the results of which are shown in Fig. 7. Fig. 7a shows SEM micrograph of the analyzed area. The maps in Fig. 7b and c do not show visible anomalies in the distribution of Mg which is uniformly distributed in the matrix and Cr which is primarily concentrated in the Cr_2O_3 particles. Similarly oxygen (O) (Fig. 7d) seems to be primarily concentrated in the Cr_2O_3 particles. However, the XRD pattern Fig. 2b, registered after 150 desorption/absorption cycles (after final absorption), shows no diffraction peaks of Cr_2O_3. It also shows a weak and broad peak of MgO but does not show any peaks of metallic Cr that would indicate some reduction of Cr_2O_3 to Cr and MgO. On the other hand, XPS measurement in Fig. 8a shows no presence of Cr before cycling and the presence of a small spectrum of Cr in Fig. 8b after 150 cycles. Taking into account all these observations it seems that the reduction of Cr_2O_3 during long-term cycling has indeed occurred but the amount of reduced Cr seems to be small and may not be clearly resolved by XRD. Nevertheless, the issue of a partial reduction of chromium oxide observed by XPS still needs more research in order to establish unambiguously if this factor may, indeed, have such a remarkable influence on the

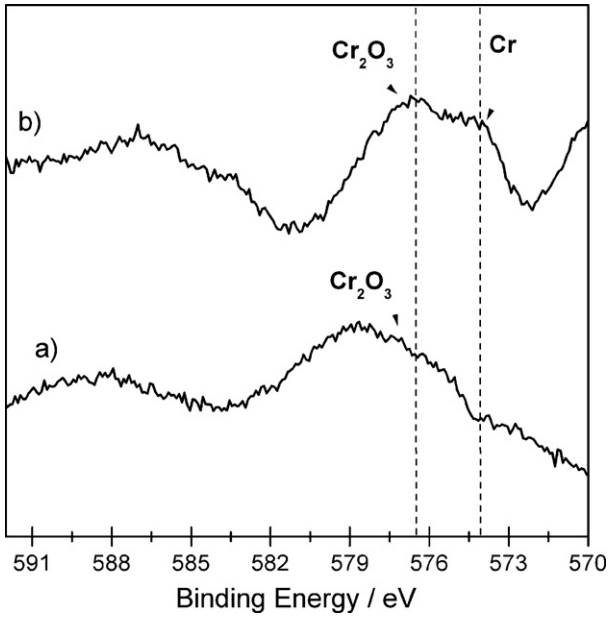

Fig. 8. XPS spectrum measured for a sample (a) before and (b) after 150 cycles.

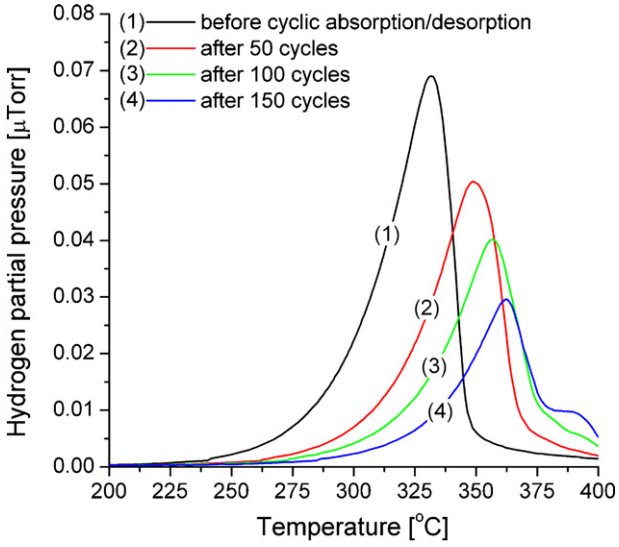

Fig. 9. TPD hydrogen desorption spectra measured before and after cycling at 325 °C for 50, 100 and 150 cycles recorded with the heating rate of 20 °C/min.

decrease of hydrogen storage capacity with increasing number of cycles in Figs. 3 and 4.

For the sake of clarity it must be mentioned that Dehouche et al. [9] reported an increase of hydrogen storage capacity upon cycling up to 1000 cycles at 300 °C. They argued that on one hand, the kinetics of desorption are getting lower (which they observed) as the Mg/MgH_2 grain/crystallite size increases but on the other hand, larger grains/crystallite sizes mean that there is a higher volume of crystalline matter which stores larger amounts of hydrogen and less of disordered grain boundary regions which store only small amounts of hydrogen. However, assuming that nanograins/crystallites are simple cubes and the grain boundary width is approximately 0.5 nm one can estimate that for the grain size of 21 nm which was reported by Dehouche et al. [9] after milling the volume fraction of grain boundaries will be only about 14%, i.e., already pretty low. Increase of the grain size to 84 nm after 1000 cycles at 300 °C as reported by Dehouche et al. [9] reduces this value to about 3.5%. Whether or not a difference between 14 and 3.5% of grain boundary volume would have such a profound effect on the absorption/desorption rates and/or decrease/increase of hydrogen storage capacity upon cycling remains to be seen. Nevertheless, in the present work we clearly observe a decrease in the hydrogen capacity with cycling which cannot be explained as proposed by Dehouche et al. [9].

In order to have an additional insight into the effect of microstructural changes on the rate of transformation upon cycling, TPD tests with the heating rate of 20 °C/min were carried out which are shown in Fig. 9. It is clearly seen that the temperature maxima of TPD curves are shifted to higher temperature range with increasing number of cycles. Also a formation of an additional peak is observed after 150 cycles which may be due to the sintering of particles into larger agglomerates which affect the shift of desorption temperature to higher temperatures.

In conclusion, one must say that the major microstructural changes observed upon cycling such as sintering of individual powder particles into agglomerates (Fig. 5), segregation of the Cr_2O_3 particles (Fig. 5), increase in grain/crystallite growth (Fig. 6) and finally some reduction of Cr_2O_3 to Cr and MgO all seem to be responsible for the decrease of hydrogen storage capacity upon cycling (Fig. 3). However, it is hard to establish unambiguously at the moment which microstructural change is a predominating one. These microstructural alterations reduce the overall rate of transformation as observed by a shift of TPD curves to higher temperature range (Fig. 9).

4. Conclusions

A nanocomposite of MgH_2 with 10 wt.% of Cr_2O_3 nanopowder catalyst (particle size <50 nm) was synthesized by ball milling for 1 h in a Fritsch P6 planetary ball mill with the resulting grain size of β-MgH_2 equal to ~30 nm. Subsequently, the nanocomposite was subjected up to 150 desorption/absorption cycles at 325 °C. PCT curves obtained at 325 °C after every 25 cycles clearly show a gradual loss of hydrogen storage capacity upon cycling from ~5.2 wt.% after 1 cycle to ~4.6 wt.% after 150 cycles. Microstructural investigations of a sample after 150 cycles carried out by XRD, STEM and XPS techniques show a substantial sintering of initially individual MgH_2/Mg powder particles, segregation of the Cr_2O_3 particles to the interfaces between the sintered Mg particles and the grain/crystallite growth to the sizes larger than 100 nm in the agglomerated particles. Some degradation of the catalyzing Cr_2O_3 particles by the reduction of Cr_2O_3 by Mg with the resulting formation of metallic Cr and MgO is also observed after 150 cycles. TPD curves are shifted to higher temperature range with increasing number of cycles. Therefore, those major microstructural changes observed upon cycling all seem to be responsible for the reduction of hydrogen storage capacity upon cycling and the reduction of the overall rate of transformation.

Acknowledgement

This work was financially supported by the Polish Ministry of Science and Higher Education, Key Project POIG.01.03.01-14-016/08 which is gratefully acknowledged.

References

[1] http://www.nuvera.com/products/androm.php.
[2] R.A. Varin, T. Czujko, Z. Wronski, Nanomaterials for Solid State Hydrogen Storage. Sec. 1.4.2, Springer, New York, 2009.
[3] B. Bogdanović, K. Bohmhammel, B. Christ, A. Reiser, K. Schlichte, R. Vehlen, U. Wolf, J. Alloys Compd. 282 (1999) 84–92.

[4] B. Bogdanović, H. Hofmann, A. Neuy, A. Reiser, K. Schlichte, B. Spliethoff, S. Wessel, J. Alloys Compd. 292 (1999) 57–71.
[5] M. Polanski, J. Bystrzycki, T. Plocinski, Int. J. Hydrogen Energy 33 (2008) 1859–1867.
[6] T. Klassen, in: R.H.J. Hannink, A.J. Hill (Eds.), Nanostructure Control of Materials, Woodhead Publ. Ltd., Cambridge, England, 2006.
[7] R.A. Varin, T. Czujko, Z.S. Wronski, Int. J. Hydrogen Energy 34 (2009) 8603–8610.
[8] B. Paik, A. Walton, V. Mann, D. Book, I.P. Jones, I.R. Harris, Int. J. Hydrogen Energy 35 (2010) 9012–9020.
[9] Z. Dehouche, T. Klassen, W. Oelerich, J. Goyette, T.K. Bose, R. Schulz, J. Alloys Compd. 347 (2002) 319–323.